Multiscale Transient Thermal, Hydraulic, and Mechanical Analysis Methodology of a Printed Circuit Heat Exchanger Using an Effective Porous Media Approach

Eugenio Urquiza[1]
Thermotive LLC,
8415 Fredericksburg Rd Suite 402,
San Antonio, TX 78229
e-mail: keno@cal.berkeley.edu

Kenneth Lee
Department of Mechanical Engineering,
University of California,
6141 Etcheverry Hall,
Berkeley, CA 94720

Per F. Peterson
Department of Nuclear Engineering,
University of California,
4155 Etcheverry Hall, MC 1730,
Berkeley, CA 94720

Ralph Greif
Department of Mechanical Engineering,
University of California,
6107 Etcheverry Hall, Mailstop 1740,
Berkeley, CA 94720

Printed circuit heat exchangers (PCHE) and the similar formed plate heat exchangers (FPHE) offer highly attractive economics due to their higher power densities when compared to more conventional shell-and-tube designs. However, their complex geometry makes them more vulnerable to damage from thermal stresses during transient thermal hydraulic conditions. Transient stresses far exceed those predicted from steady state analyses. Therefore, a transient, hydraulic, thermal, and structural analysis is needed to accurately simulate and design high performing PCHE. The overall length of the heat exchanger can be thousands of times larger than the characteristic length for the heat transfer and fluid flow. Furthermore, simulating the thermal hydraulics of the entire heat exchanger plate is very time consuming and computationally expensive. The proposed methodology mitigates this by using a multiscale analysis with local volume averaged (LVA) properties and a novel effective porous media (EPM) approach. This method is implemented in a new computer code named the compact heat exchanger explicit thermal and hydraulics (CHEETAH) code which solves the time-dependent, mass, momentum, and energy equations for the entire PCHE plate as well as hot and cold fluid streams using finite volume analysis (FVA). The potential of the method and code is illustrated with an example problem for a Heatric-type helium gas-to-liquid salt PCHE with offset strip fins (OSF). Given initial and boundary conditions, CHEETAH computes and plots transient temperature and flow data. A specially developed grid mapping code transfers temperature arrays onto adapted structural meshes generated with commercial FEA software. For the conditions studied, a multiscale stress analysis reveals mechanical vulnerabilities in the HX design. This integrated methodology using an EPM approach enables multiscale PCHE simulation. The results provide the basis for design improvements which can minimize flow losses while enhancing flow uniformity, thermal effectiveness, and mechanical strength. [DOI: 10.1115/1.4024712]

Keywords: printed circuit heat exchanger, formed plate heat exchanger, compact heat exchanger, heat transfer, offset strip fin, transient, porous media, thermal stress, liquid salt, high temperature, nuclear power, Generation IV, solar thermal

1 Introduction

High temperature heat transfer systems are fundamental to the economical and successful deployment of many emerging power generation technologies. Temperatures between 800 and 1000 °C can be used to chemically separate hydrogen from oxygen in water via the sulfur iodine cycle. Alternatively, a multiple reheat helium Brayton cycle can convert energy at these temperatures to electricity with efficiencies near 50% [1,2]. Plant designs often include an intermediate heat transfer loop with heat exchangers at either end to transfer thermal energy at high temperature from a nuclear reactor, solar concentrator, or other heat source to a power or thermochemical plant located nearby [1–7]. Liquid salts and inert gases such as helium are proposed as heat transfer fluids for various high temperature applications including new nuclear power plant concepts.

PCHE are strong candidate heat exchangers for these intermediate loops because they can achieve much higher power density with far less material than a comparable shell-and-tube heat exchanger [8]. The high temperatures in the intermediate loop require the use of a heat exchanger that retains its strength at high temperatures. Even ceramic heat exchangers are being considered for this purpose [9]. The PCHE is fabricated from flat plates into which fluid flow channels are chemically milled or etched. Separate plate geometries are designed and fabricated to carry the cold and hot fluids. These plates are arranged in an alternating cold, hot, cold, hot alternating stack and are diffusion-bonded together.

Diffusion-bonding is a solid-state joining process where the plate stack becomes a solid block of metal. The bonding process involves pressing plates together at elevated temperatures over an extended period of time until grains grow between the plates, essentially eliminating the interface and creating a diffusion bond [8,10]. Unlike brazed heat exchangers that are limited by the properties of the weaker brazing material, the diffusion-bonding process yields an entire heat exchanger with the strength of the base material [5]. This is particularly important in high temperature

[1]Corresponding author.
Manuscript received February 7, 2013; final manuscript received April 4, 2013; published online October 3, 2013. Assoc. Editor: Jovica R. Riznic.

applications where strength is reduced and creep resistance is important thereby requiring exotic and costly alloys.

Although these types of heat exchangers can achieve high effectiveness, they can also be susceptible to very large thermal stresses that occur during flow transients. These stresses are significantly higher than those predicted under steady state conditions. Peak stresses occur at the feature scale where the fin roots and the flow channel geometry concentrate stresses resulting from thermal expansion at the plate scale. Determining transient plate scale temperature distribution with feature scale heat transfer phenomena requires a multiscale thermal, hydraulic, and mechanical methodology. The methodology proposed in this work is applicable to all PCHE. The example presented is of a new heat exchanger design (Heatric-type) that enhances heat transfer with rounded OSF.

2 High Temperature Heat Exchanger Design Process

CHEETAH code is unique in that it is specifically designed to simulate and analyze the transient, cross, and counter-flow (or parallel-flow) conditions occurring between the plates of a PCHE. Some commercial codes can analyze parts of the PCHE in high resolution, but only CHEETAH is designed to solve transient temperature distributions over an entire PCHE plate, providing results that are essential in determining plate scale transient thermal stresses.

The major components of the multiscale analysis method proposed are shown schematically in Fig. 1. Data input into CHEETAH begins with LVA of the pertinent thermal hydraulics properties at the feature scale. These include fin shapes, channel geometry and dimensions that are utilized in the friction and Colburn factor calculations. Without LVA, the transient analysis of this multiscale system would be very time consuming and computationally expensive. In the hydraulic analysis, CHEETAH applies an EPM formulation within an iterative calculation procedure. In the first iteration initial and boundary conditions lead to the calculation of the first flow distribution. This is then utilized in the energy balance which determines the first iteration's calculated temperature distribution. The temperature distribution is then utilized to determine the temperature-dependent fluid properties which are then utilized to determine the flow distribution in the second iteration.

The designer begins with a baseline PCHE design and uses flow and temperature data calculated with the code to make informed design decisions. The designer may decide to redesign the manifolds, fins or channels, shapes and profiles in the PCHE and then simulate the new PCHE design to evaluate the effect on performance. When the code provides flow fields, temperature arrays, and a PCHE thermal effectiveness that meets performance criteria, the design process proceeds to the thermomechanical or structural performance of the PCHE.

Effective or LVA structural properties (Young's, Poisson's, shear moduli) are found by analyzing a heat exchanger plate's representative unit cells with a commercial FEA code. These effective properties are applied to the plate model's structural mesh properties. The temperature distribution is then mapped onto the structural plate model for thermal stress analysis at both the plate and feature scale. If the steady state stress analysis gives acceptable results then thermal transient data from CHEETAH can be used to calculate transient thermal stresses like those associated with flow and temperature transients resulting from valve movements, pump trips, or shut downs. The proposed multiscale methods of analysis can be used in conjunction with the CHEETAH code and commercial structural FEA codes to iteratively analyze, improve, and enhance heat exchanger design and performance.

3 Thermal Hydraulic Methodology

3.1 Hydraulics and EPM Assumption. The EPM method uses a Darcy formulation for the velocities to determine the flow in the manifolds and OSF regions of a composite plate including geometry from both fluid carrying plates in the PCHE. In this example, the method is applied to an OSF heat exchanger. In this geometry a new boundary layer is created at the leading edge of each fin and subsequently altered in the mixed flow that occurs in its wake. The periodically repeating fin geometry in the plate creates mixing and crossflow; this makes the EPM treatment especially appropriate [4].

Manglik and Bergles [11] offer a good friction factor fit for the OSF heat exchanger arrangement over a wide range of Reynolds numbers. OSF heat exchangers were originally developed to be fabricated through brazing and with fins made from stamped sheet metal. The fins proposed in this example are thicker, more appropriate for diffusion-bonding process, and have a rounded profile to reduce flow losses. The OSF heat exchanger plate and fin geometry are shown in Figs. 2 and 3.

The EPM method discretizes using mesh sizes roughly the size of the geometry's hydraulic diameter. Increasing the grid size greatly reduces the computational resources required to analyze transient behavior in a large and complex heat exchanger plate. In this case the maximum grid size is limited by the manifold geometry and flow paths. Furthermore, the grid size and time-step determine the numerical stability via the Courant–Friedrichs–Lewy (CFL) condition [12].

3.1.1 Determining the Effective Permeability. The effective permeability is the critical parameter needed for the hydraulic

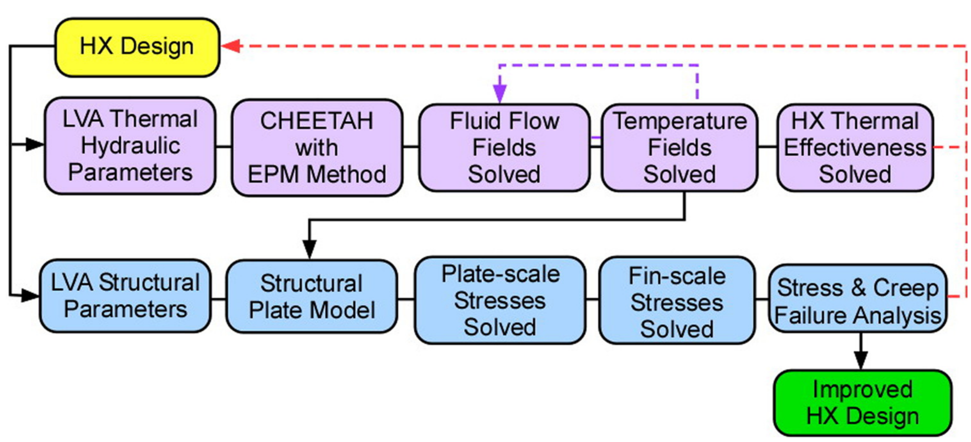

Fig. 1 Heat exchanger design optimization process enabled using CHEETAH and the EPM method

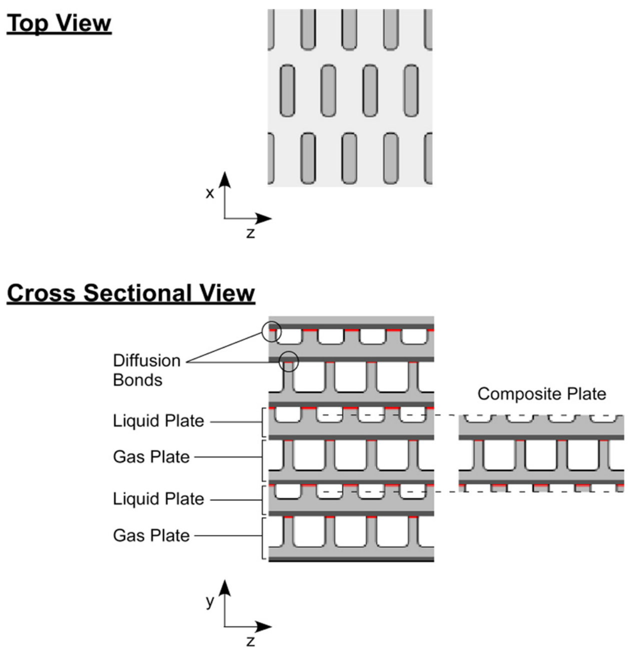

Fig. 2 Cut-away view through the OSF section showing alternating liquid and gas flow channels. Dark bands at the top of each fin indicate the location of diffusion-bonded joints between the plates.

analysis of the PCHE. It is determined via local volume averaging using the EPM assumption. Extensive analytical and experimental work has characterized the hydraulic properties of many OSF geometries. Kays and London, Shah, Webb and others have published a large body of correlations for the fluid flow and heat transfer characteristics of heat exchangers. Kays and London in particular published many correlations specifically for compact heat exchangers. In addition to the fin geometry, the flow regime and manufacturing methods used in making the fins also affect pressure drop and heat transfer in the PCHE [13].

The Fanning friction factor is used to determine the pressure losses due to friction in the flow over widely varying conditions. It is also used here to determine the medium's effective permeability. This porous media characterization is such that the void fraction, or porosity, is unique to each side of the PCHE plate and thus unique to the plates holding each of the two fluids. The hot and cold fluids are kept completely separate with each moving through parallel channels or pore networks in the plates while exchanging energy, but not mass.

Geometric symmetry between plates greatly simplifies the subsequent structural analysis and creates adiabatic planes in the energy balance. For this purpose, a composite plate is created. It is simply a plate that contains the geometrical features of both the hot and cold plates in a symmetrical arrangement as shown in the cross sectional view of Fig. 2. The composite plate has an orthotropic (X and Z) permeability for each fluid phase in the flow plane. Instead of a void fraction or porosity, each entity has a phase fraction ϕ which varies with the local geometry in the PCHE. The three-phase fractions sum to unity with its subscript describing the entity (fluid cold, solid, or fluid hot). The Darcy velocity u_{D} is the interstitial velocity multiplied by the phase fraction.

Darcy's equation is modified by Urquiza [4] and used as a modified momentum equation for the EPM approximation

$$u_{\mathrm{D}} = -\frac{D_{\mathrm{h}x}\mu\phi^2}{2f_{\mathrm{f}x}\rho u_{\mathrm{D}}}\frac{1}{\mu}\frac{d\Phi}{dx}, \quad w_{\mathrm{D}} = -\frac{D_{\mathrm{h}z}\mu\phi^2}{2f_{\mathrm{f}z}\rho w_{\mathrm{D}}}\frac{1}{\mu}\frac{d\Phi}{dz} \tag{1}$$

Thus, the directional effective permeability, k, on the hot and cold side can be found in terms of the Fanning friction factor, f_{f}:

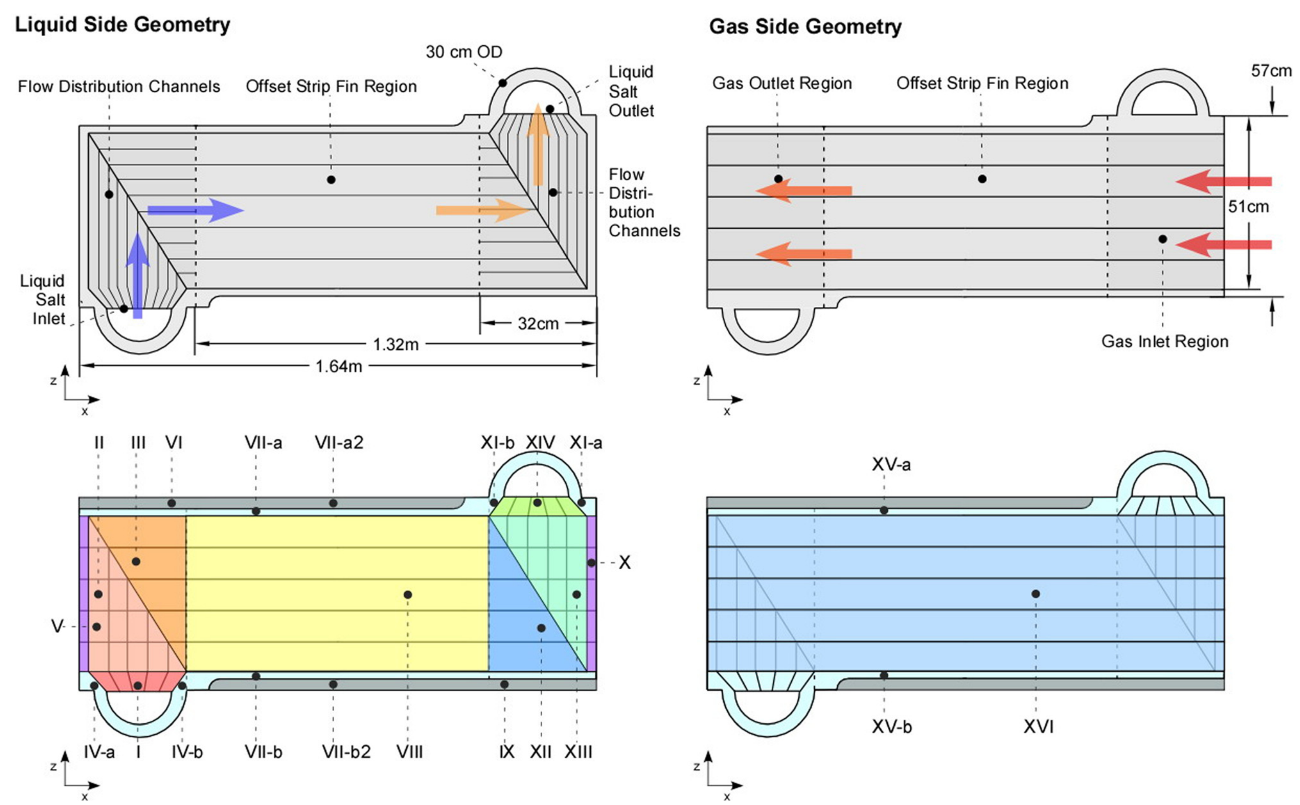

Fig. 3 Zones in the composite plate with varying thermal and hydraulic properties

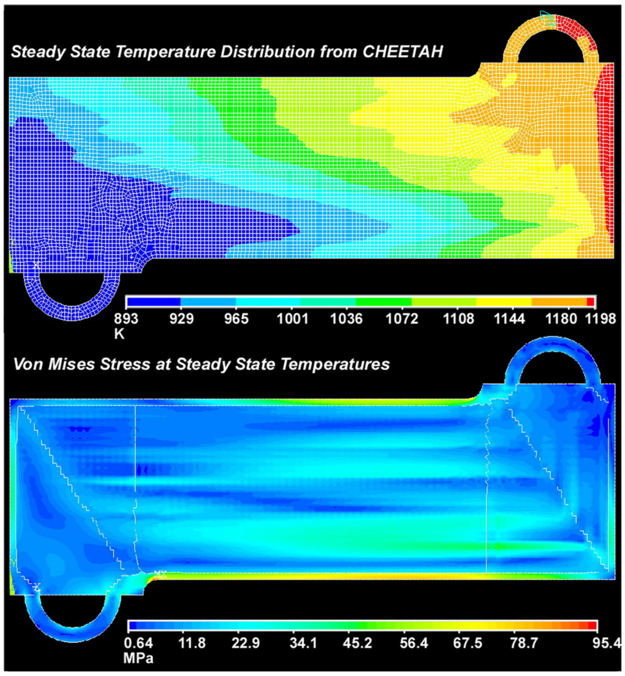

Fig. 4 The steady state temperature and corresponding stress distribution

$$k_x = \frac{D_{hx}\mu\phi^2}{2f_{fx}\rho u_D}, \quad k_z = \frac{D_{hz}\mu\phi^2}{2f_{fz}\rho w_D} \tag{2}$$

Fanning friction factor, and thus the permeability, is velocity dependent for higher Reynolds number flows. The expected average velocity of the fluid flow is used as an initial condition to calculate the local permeabilities of the plates. These values are determined from mass flow rates determined from component sizing calculations. The assignment of the permeability array depends on the local PCHE geometry, which is divided into distinct zones as shown in Fig. 3. The same zones are used to designate the LVA heat transfer coefficients.

With a permeability array specified within CHEETAH, the code iteratively solves for the pressure distribution using an explicit scheme and prescribed inlet and outlet pressures as boundary conditions. Then, fluid velocity is calculated for each fluid at the boundaries of thousands of finite volumes. This creates a velocity field or array for each fluid in the PCHE composite plate using the same equation in OSF flow zones, manifolds, near the boundaries, and to achieve no flow in the impermeable areas. The values of the permeability array change slightly with temperature-dependent thermophysical properties and the local fluid velocity.

3.2 Thermal Analysis. This thermal analysis is focused on the larger plate scale, but the heat transfer properties can be determined using computational analysis on the feature scale. Analysis on feature scale effects would focus on fin geometry and the periodic thermal-boundary layers and wakes created in the interrupted flow by the OSF. The variation of the convection coefficient over the length of the fin row has been studied to improve fin shape and spacing. A study investigating phenomena at this scale has been performed using a CFD code by Subramanian at UNLV [14]. Hu and Herold have also published work examining the effects of Prandtl number on pressure drop, on heat transfer and on the length of the developing region in the OSF zone as determined using the Graetz number [15].

In addition to the effective permeability, other LVA properties used in the EPM method include the hydraulic diameter, effective

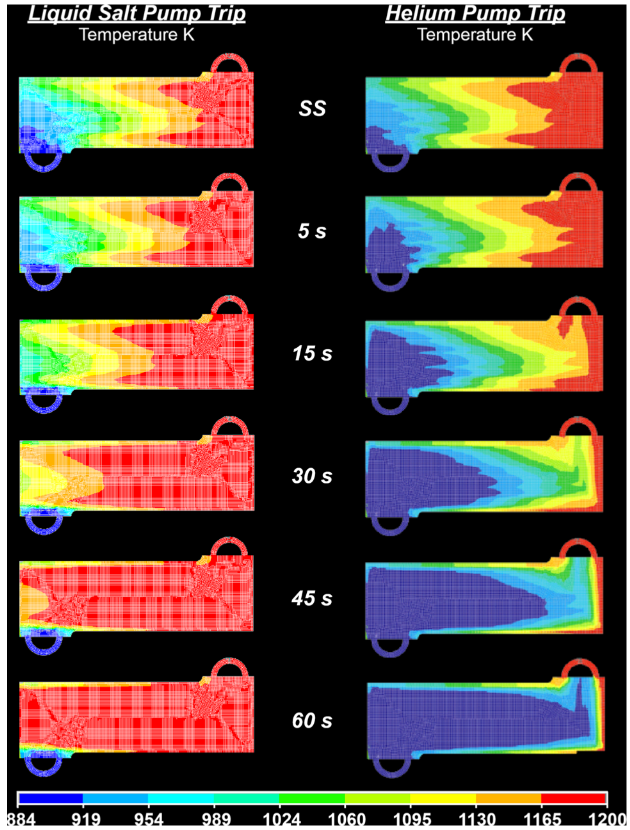

Fig. 5 Transient temperature distributions solved by CHEETAH for the composite plate of the PCHE after a step change in flow rate initiates a thermal hydraulic transient

directional conductivity, heat transfer surface area density, and the convective heat transfer coefficient. LVA heat transfer properties such as the convection coefficient come from geometry-specific correlations. Other LVA heat transfer properties such as surface area and effective thermal conductivity are calculated with CAD and FEA software by Urquiza [4]. In the example presented, CHEETAH calculates and assigns the effective permeability as a LVA property using characteristic fin and channel ratios with the Colburn factor correlation by Manglik and Bergles [11].

Solving the mass balance and Darcy equations yields the velocity arrays for both phases present in the PCHE. With this information the code solves the energy equations for every control

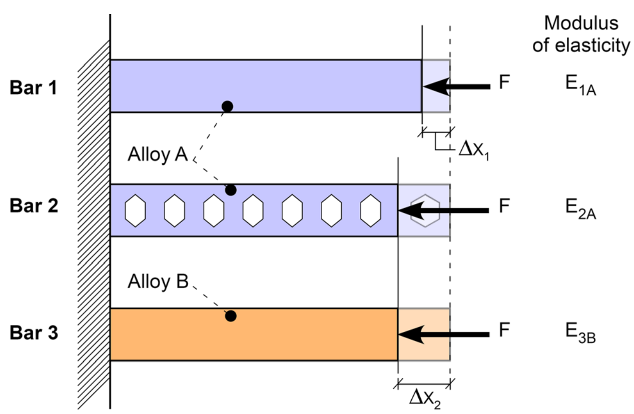

Fig. 6 The strain of a mechanical component with a complex geometry can be replicated with a component with a simple geometry when the two share effective mechanical properties such as an effective modulus of elasticity

volume in the PCHE over discrete time steps using an explicit FVA method. In the stack or y-direction there is one control volume per phase —cold fluid, solid (i.e., porous medium or composite plate), and hot fluid. The implementation of the FVA method in the code is covered in detail by Urquiza [4].

The elliptical partial differential equations that follow describe the nondimensional energy conservation equations on a differential element for each phase in the heat exchanger.

Heat transfer equations:

Hot fluid (fh):

$$-u^*_{\mathrm{fh}}\frac{\partial T^*_{\mathrm{fh}}}{\partial x^*} - w^*_{\mathrm{fh}}\frac{\partial T^*_{\mathrm{fh}}}{\partial z^*} + \frac{1}{\mathrm{Pe}_x}a''_{\mathrm{fh}x}\frac{\partial^2 T^*_{\mathrm{fh}}}{\partial x^{*2}} + \frac{1}{\mathrm{Pe}_z}a''_{\mathrm{fh}z}\frac{\partial^2 T^*_{\mathrm{fh}}}{\partial z^{*2}} - \mathrm{St}_x \cdot a'_{\mathrm{fh}s}L\cdot(T^*_{\mathrm{fh}} - T^*_{\mathrm{s}}) = \phi_{\mathrm{fh}}\frac{\partial T^*_{\mathrm{fh}}}{\partial t^*} \quad (3)$$

Solid (s):

$$\alpha_x \cdot a''_{\mathrm{s}x}\frac{\partial^2 T^*_{\mathrm{s}}}{\partial x^{*2}} - \alpha_z \cdot a''_{\mathrm{s}z}\frac{\partial^2 T^*_{\mathrm{s}}}{\partial z^{*2}} + \mathrm{St}_x \cdot a'_{\mathrm{fh}s}L\cdot(T^*_{\mathrm{fh}} - T^*_{\mathrm{s}}) - \mathrm{St}_x \cdot a'_{\mathrm{fcs}}L\cdot(T^*_{\mathrm{s}} - T^*_{\mathrm{fc}}) = \phi_{\mathrm{s}}\frac{\partial T^*_{\mathrm{s}}}{\partial t^*} \quad (4)$$

Cold fluid (fc):

$$-u^*_{\mathrm{fc}}\frac{\partial T^*_{\mathrm{fc}}}{\partial x^*} - w^*_{\mathrm{fc}}\frac{\partial T^*_{\mathrm{fc}}}{\partial z^*} + \frac{1}{\mathrm{Pe}_x}a''_{\mathrm{fc}x}\frac{\partial^2 T^*_{\mathrm{fc}}}{\partial x^{*2}} + \frac{1}{\mathrm{Pe}_z}a''_{fcz}\frac{\partial^2 T^*_{\mathrm{fc}}}{\partial z^{*2}} + \mathrm{St}_x \cdot a'_{\mathrm{fcs}}L\cdot(T^*_{\mathrm{s}} - T^*_{\mathrm{fc}}) = \phi_{\mathrm{fc}}\frac{\partial T^*_{\mathrm{fc}}}{\partial t^*} \quad (5)$$

Sufficiently high flow velocities and low thermal conductivity in the fluids often create Peclet numbers, $\mathrm{Pe} = u_{\mathrm{f}} * D_{\mathrm{h}}/\alpha$, that are sufficiently high so that some terms in Eqs. (3) and (5) can be neglected. CHEETAH solves these equations over a finite volume using an explicit scheme and very small time steps to maintain stability [4]. The stability behaves in agreement with the CFL condition [12]

$$\frac{u_{\mathrm{f}}\Delta t}{\Delta x} + \frac{w_{\mathrm{f}}\Delta t}{\Delta z} \leq C \quad (6)$$

3.3 Results. CHEETAH finds the steady state temperature distribution in the PCHE after iterating between hydraulic and thermal analyses. In this example from the advanced high temperature reactor concept, the candidate PCHX operates in a scenario where the hot fluid is high pressure helium at 7 MPa with an inlet temperature of 1200 K and the cold fluid is liquid salt near ambient pressure and with an inlet temperature of 800 K [4]. Figure 4 shows the steady state temperature distribution on the composite plate calculated with temperature-dependent thermophysical properties and the corresponding Von Mises stress distribution.

This stress distribution provides the basis for the creep failure analysis performed on this design of the PCHX composite plate. For alloy 617, HAYNES International [16] lists that at 1143 K, the maximum allowable creep stress is 47 MPa. Figure 4 shows that even the plate scale stresses exceed those allowable in zones corresponding to this temperature range in this PCHX design. The structural model leading to the plate scale stress analysis shown in Fig. 4, as well as the local stress analysis is shown in Figs. 8 and 9, are discussed in Sec. 3.4. These were calculated using the multiscale analysis and show even higher stresses due to the stress concentrating detailed geometry of the PCHX.

The allowable creep stress drops significantly at higher temperatures. Haynes lists a maximum allowable stress of only 17 MPa at temperatures of 1253 K. The peak operating temperature in this PCHX is 1200 K (927 °C), and performing a linear interpolation gives a maximum allowable sustained creep stress of 32.3 MPa in

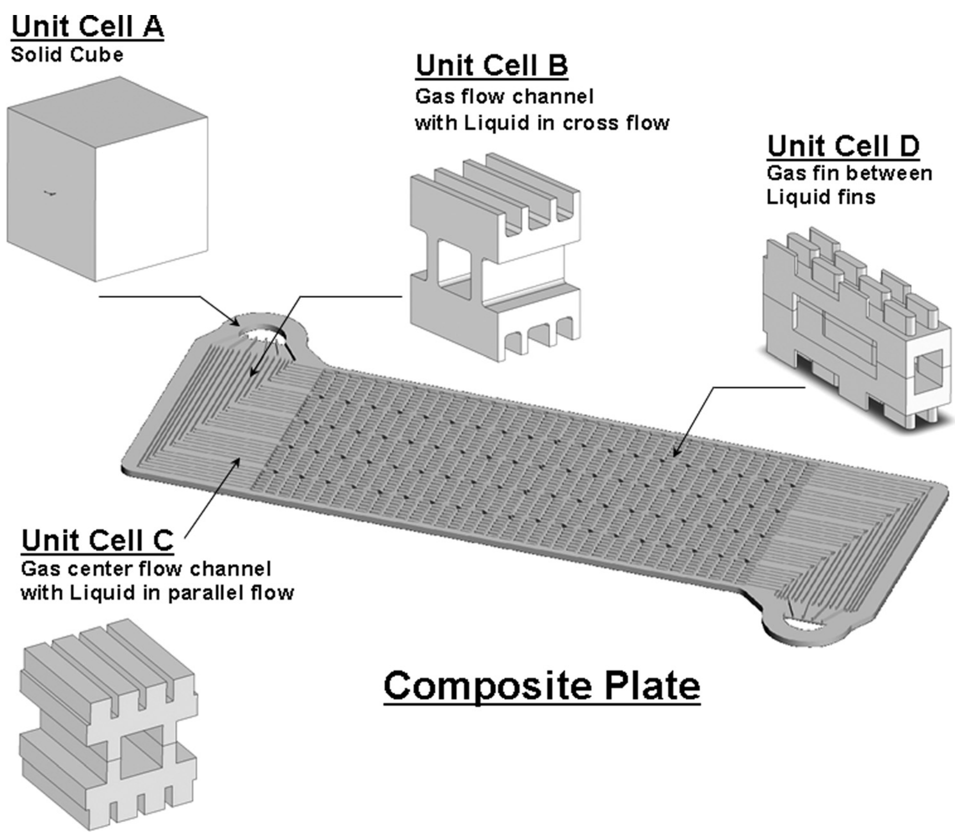

Fig. 7 The four unit cells characterizing the complex geometry of this composite plate

1200 K zones. Von Mises stresses at the plate scale for these zones also exceed the maximum allowable creep stress with no margin.

The analysis in Fig. 4 includes only two dimensional plate scale stresses and therefore excludes the pressure differential between the liquid and gas phases. This pressure differential is 7 MPa in this application, so with the plate scale stresses included the total stress would increase further. Clearly the creep stresses in this design are unacceptable for the application; the plate features must be redesigned to reduce nominal operating stresses. This indicates that local or fin-scale stresses, which tend to be higher, will likely fail the creep criteria as well.

Transient thermal hydraulic solutions from CHEETAH code for a PCHE plate experiencing a pump trip are analyzed in detail by Urquiza using the methods presented [4]. Solutions for the transient temperature distributions in a PCHE heat exchanger with OSF start from a nominal operational state and then undergo a cold side pump trip (Fig. 5 left) and a hot-side pump trip (Fig. 5 right).

3.3.1 Verification of Numerical Method. The transient response of a three-phase system in two spatial dimensions undergoing changes in flow rate represents a challenging verification problem. Due to its new capabilities, the results of full CHEETAH code for this example problem could not be fully verified. However, a simplified one dimensional transient version of CHEETAH has been tested and verified under many conditions. For example, CHEETAH 1D duplicates steady state analytical solutions with excellent agreement. The code also analyzed several two fluid, 1D thermal hydraulic transients studied by Yin and Jensen [17]. All transient temperature profiles replicated Yin and Jensen's Dymola results showing no discrepancies. Furthermore, Yin and Jensen benchmarked their numerical results against those of Romie [18] and Roetzel and Xuan [19] for a parallel and counter-flow heat exchanger arrangement also reporting excellent agreement [17]. The match between the results of the CHEETAH 1D code and those from Yin and Jensen's Dymola analysis verifies CHEETAH 1D. While this does not verify the results of the full version of CHEETAH, it does provide confidence in the underlying methods and algorithms. The computational verification is covered in detail by Urquiza [4].

3.4 Multiscale Structural Analysis. The approach to the multiscale structural analysis is illustrated conceptually by the example in Fig. 6. The purpose of the LVA properties is to obtain plate scale principle stresses by replacing complex fin and flow channel geometry in the composite plate—analogous to bar 2—with simple geometry that reproduces the effective strain—analogous to bar 3.

Just as LVA properties were determined using zones in the thermal hydraulic analysis with CHEETAH, zones are also used to find LVA structural properties of the composite plate. The hot and cold sides of the plate are analyzed together because the symmetry of the composite plate captures both plate geometries as shown in Fig. 7. Unit cells are small representative building blocks that capture the geometry of both hot and cold plates in a PCHE. Zones in the composite plate are chosen such that their geometry can be constructed entirely out of a single unit cell. Thus, the complex structural properties of the plate are captured and can be determined by structurally analyzing each unit cell.

LVA structural properties such as Poisson ratios, elastic moduli, and shear moduli must be determined for all unit cells and applied to their zones within the composite plate model so that the plate scale stresses shown in Fig. 4 can be solved. With the exception of Unit Cell A which is isotropic, all unit cells shown in Fig. 7 exhibit orthotropic behavior. Thus, nine constants are needed to fully characterize the LVA properties including three moduli of elasticity (Young's moduli), E, three Poisson's ratios, ν, and three shear moduli, G. These constants are related to one another through Hooke's Law for orthogonal materials. The 6×1 stress matrix shown below is set equal to the product of the 9×9 inverse elastic matrix (stiffness matrix) and the 6×1 strain matrix [20]

$$\begin{Bmatrix} \sigma_{xx} \\ \sigma_{yy} \\ \sigma_{zz} \\ \sigma_{xy} \\ \sigma_{yz} \\ \sigma_{xz} \end{Bmatrix} = \begin{bmatrix} \frac{1}{E_x} & -\frac{\nu_{xy}}{E_x} & -\frac{\nu_{xz}}{E_x} & 0 & 0 & 0 \\ -\frac{\nu_{yx}}{E_y} & \frac{1}{E_y} & -\frac{\nu_{yz}}{E_y} & 0 & 0 & 0 \\ -\frac{\nu_{zx}}{E_z} & -\frac{\nu_{zy}}{E_z} & \frac{1}{E_z} & 0 & 0 & 0 \\ 0 & 0 & 0 & \frac{1}{2G_{xy}} & 0 & 0 \\ 0 & 0 & 0 & 0 & \frac{1}{2G_{yz}} & 0 \\ 0 & 0 & 0 & 0 & 0 & \frac{1}{2G_{xz}} \end{bmatrix}^{-1} \begin{Bmatrix} \varepsilon_{xx} \\ \varepsilon_{yy} \\ \varepsilon_{zz} \\ \varepsilon_{xy} \\ \varepsilon_{yz} \\ \varepsilon_{xz} \end{Bmatrix} \tag{7}$$

Furthermore, for orthotropic materials

$$\frac{\nu_{xy}}{E_x} = \frac{\nu_{yx}}{E_y}, \quad \frac{\nu_{yz}}{E_y} = \frac{\nu_{zy}}{E_z}, \quad \frac{\nu_{xz}}{E_x} = \frac{\nu_{zx}}{E_z} \tag{8}$$

This leaves nine unknown parameters for a given state of stress and strain. The LVA structural parameters are determined by FEA of each unit cell under known shear and orthogonal strains as shown in detail previously by Huang [21] and also by Urquiza [4]. Finding the LVA structural properties for the unit cells and assigning them to their corresponding zones in the composite plate enables FEA thermal stress analysis of the composite plate.

Using a specially developed interface code in MATLAB, the temperature field from CHEETAH is mapped onto the structural mesh produced by the FEA software—ANSYS 11. With the LVA structural properties and the coefficient of thermal expansion for the plate material—Alloy 617, in this example—assigned to the composite plate and a minimal one node constraint, the plate scale thermal stress analysis resolves the stress distribution, shown in Fig. 5. Likewise, the FEA calculates the maximum principle stresses in each of the zones corresponding to the unit cells. By then, imposing these principle stresses on separate detailed meshes for each unit cell, the local peak stresses can be reproduced. Local stresses peak in the OSF region 30 s into the thermal

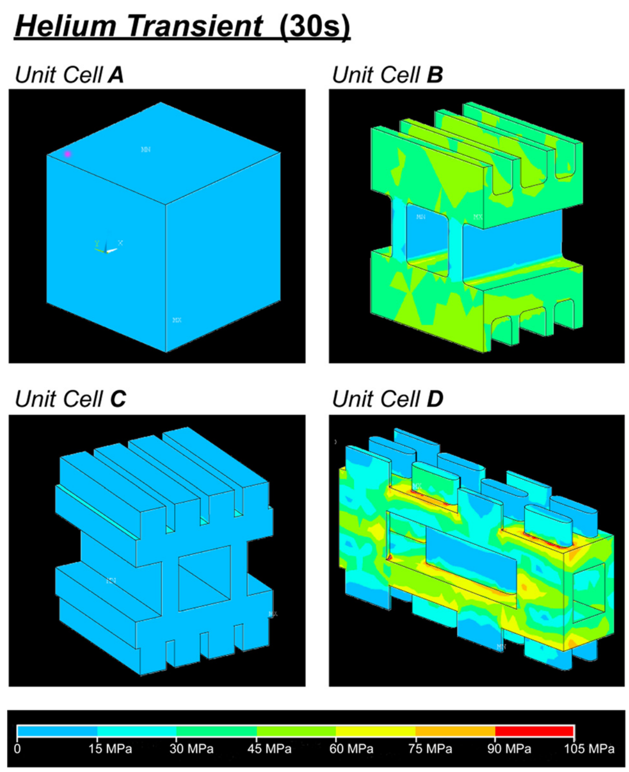

Fig. 8 Local peak stresses on unit cells in the PCHX during a simulated thermal transient involving loss of forced gas heating

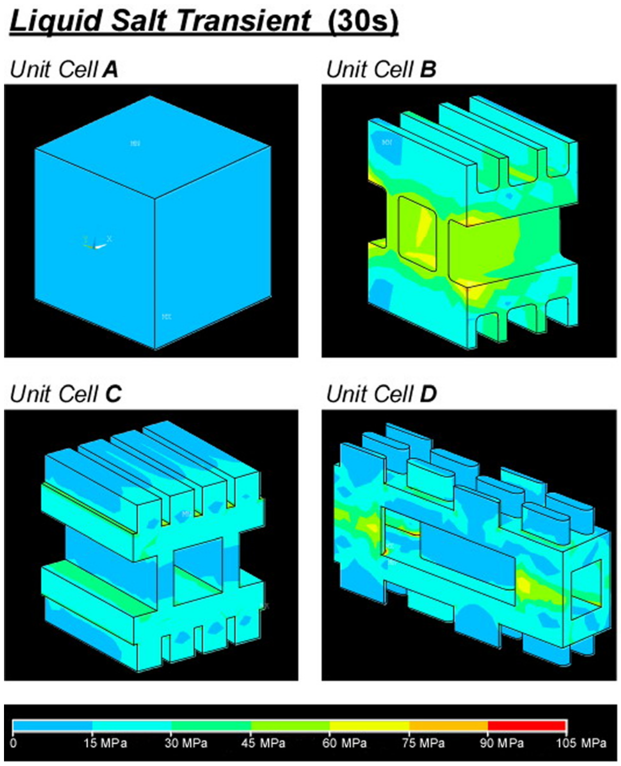

Fig. 9 Local peak stresses on unit cells in the PCHX during a simulated thermal transient involving loss of forced liquid cooling

hydraulic transients. Figures 8 and 9 show stresses that exceed yield stresses at fin roots in this PCHX design. While this failure mode could be mitigated with fillets at the roots and flywheels on the pumps to reduce the shock of pump trips, managing the creep stresses is significantly more daunting. Urquiza also shows detailed transient thermal stresses on both the plate and feature scale for cold and hot-side pump trips [4].

4 Conclusions

Despite the attractiveness associated with running a PCHE at high temperature, the operational limits of a PCHE can be difficult to determine. This is partly because accurate transient thermal, hydraulic, and mechanical simulation of these critical devices is complex and computationally expensive. Simplified steady state stress analyses significantly underpredict the peak stresses occurring during thermal hydraulic transients and empirical testing of these devices is often cost prohibitive.

The EPM method and its implementation in CHEETAH code bridges multiple scales and provides thermal, hydraulic, and mechanical results at both component and feature scales. For the first time, an EPM method enables the transient thermal hydraulic and structural computation of a PCHE containing features too small to discretize individually. By treating the entire PCHE as an EPM, the CHEETAH code is able to capture geometry effects and calculate temperature-sensitive flow fields with significantly reduced computational effort. LVA properties also enable fast computation of energy balances resulting in transient temperature distributions in the PCHE plate, hot, and cold fluids. These results can be used for targeted thermal hydraulic improvements to HX performance such as improving overall thermal effectiveness and improving uniformity of the flow field caused by manifold geometry and temperature-dependent thermophysical properties.

After using structural submodeling to determine effective mechanical properties in the unit cells, plate scale stresses can be solved using CHEETAH's thermal hydraulic results. The principle stresses on the composite plate can then be reapplied to find local, feature scale peak stresses which can predict failure in both steady state operation and during thermal hydraulic transients. The steady state results can also be used to evaluate performance with respect to creep, which can lead to flow channel deformation and degrade effectiveness over time.

The successful application of the EPM method in CHEETAH to the example problem shows the potential of carefully undertaken volume averaging [4]. The EPM method used in CHEETAH together with structural FEA software can help designers and researchers analyze and optimize the thermal, hydraulic, and mechanical performance of a PCHE. This in turn presents a unique opportunity to improve power and chemical plant efficiency because detailed simulation and understanding of the limits of these devices buttresses next generation power plant design. When applied to existing devices, this method of analysis can help engineers estimate optimal operational conditions.

Acknowledgment

Nuclear Hydrogen Initiative (NHI) managed by UNLV; FY 07: N-ID07SS0109—University of California, Berkeley; FY 08: N-ID07SS0103—University of California, Berkeley; Chevron-Berkeley Energy Fellowship 2007; Alfred P. Sloan Foundation; and Columba Gonzalez-Quintanilla.

Nomenclature

D_h = hydraulic diameter, m
Fo = Fourier Number, dimensionless
Gz = Graetz number, dimensionless
L = characteristic length, m
Nu = Nusselt number, dimensionless
P = pressure, Pa
Pe = Peclet number, dimensionless
Pr = Prandtl number, dimensionless
Re = Reynolds number, dimensionless
St = Stanton number, dimensionless
T = temperature, K
a' = surface area density, m^2/m^3
a'' = dimensionless surface area Adx, m^3/m^3
C = an empirical constant
c_p = the specific heat, $J/(kg\ K)$
f_f = Fanning friction factor, dimensionless
h = convective heat transfer coefficient, $W/(m^2K)$
j = Colburn Factor, St $Pr^{2/3}$ or Nu/(Re$Pr^{1/3}$), dimensionless
k = effective permeability, m^2
t = thickness of the fins in the offset strip fin arrangement, m
$\bar{u}$ = average velocity, m/s
u = velocity in the x direction, m/s
u_D = Darcy velocity in the x direction, m/s
u_{int} = interstitial velocity in the x direction, m/s
x = coordinate in the flow direction
w = velocity in the z direction, m/s
z = coordinate in the cross-flow direction

Greek Symbols

α = thermal diffusivity
Δ = discrete change
ϕ = phase fraction
Φ = flow potential, Pa
μ = dynamic viscosity, Pa s
ρ = density, kg/m^3

Subscripts

c = constant
f = fluid

fc = cold fluid
fcs = between cold fluid and solid
fcx = cold fluid x direction
fcz = cold fluid z direction
fh = hot fluid
fhs = between hot fluid and solid
fh$x$ = hot fluid x direction
fh$z$ = hot fluid z direction
s = solid
sfc = between solid and cold fluid
x = x direction
z = z direction

Superscript

$*$ = nondimensional

Index Variables

i = index in the x direction (flow direction)
j = index in the y direction
k = index in the z direction (cross-flow direction)

Abbreviations

PCHE = printed circuit heat exchanger
FPHE = formed plate heat exchanger
AHTR = advanced high temperature reactor
LVA = local volume averaged
CFD = computational fluid dynamics
CHEETAH = compact heat exchanger explicit thermal and hydraulics code
EPM = effective porous media
FEA = finite element analysis
FVA = finite volume analysis
IHX = intermediate heat exchanger
OSF = offset strip fin

References

[1] Peterson, P. F., 2003, "Multiple-Reheat Brayton Cycles for Nuclear Power Conversion With Molten Coolants," Nucl. Technol., **155**, pp. 279–288. Available at: http://www.ans.org/store/j_3445

[2] Zhao, H., and Peterson, P. F., 2007, "Optimization of Advanced High-Temperature Brayton Cycles With Multiple Reheat Stages," Nucl. Technol., **158**, pp. 145–157. Available at: http://www.ans.org/store/j_3832

[3] Urquiza-Fernández, E., Peterson, P. F., and Greif, R., 2007, "Multi-Scale Thermal Analysis for Compact Plate-Type Heat Exchangers," American Institute of Chemical Engineering Annual Meeting, Salt Lake City, UT.

[4] Urquiza, E., 2009, "Transient Thermal, Hydraulic, and Mechanical Analysis of a Counter Flow Offset Strip Fin Intermediate Heat Exchanger Using an Effective Porous Media Approach," Ph.D. dissertation, Department of Mechanical Engineering, University of California, Berkeley, CA.

[5] Dewson, S. J., and Thonon, B., 2003, "The Development of High Efficiency Heat Exchangers for Helium Gas Cooled Reactors," International Congress on Advances in Nuclear Power Plants, ICAPP Paper No. 3213.

[6] Williams, D. F., Toth, L. M., and Clarno, K. T., 2006, "Assessment of Candidate Molten Salt Coolants for the Advanced High-Temperature Reactor (AHTR)," Oak Ridge National Laboratory, Oak Ridge, TN, Report No. ORNL/TM-2006/12.

[7] Peterson, P. F., Zhao, H., Niu, F., Wang, W., Schmidt, J., and Schulte-Fischedick, J., 2006, "Development of C-Sic Ceramic Compact Plate Heat Exchangers for High Temperature Heat Transfer Applications," AICHE Annual Meeting.

[8] Heatric, http://www.heatric.com/diffusion_bonded_exchangers.html

[9] Schmidt, J., Scheiffele, M., Crippa, M., Peterson, P. F., Urquiza, E., Sridharan, K., Olson, L. C., Anderson M., H., Allen T. R., and Chen, Y., 2011, "Design, Fabrication, and Testing of Ceramic Plate-Type Heat Exchangers With Integrated Flow Channel Design" Int. J. Appl. Ceram. Technol., **8**(5), pp. 1073–1086.

[10] Li, X., Kininmont, D., Le Pierres, R., and Dewson, S. J., 2008, "Alloy 617 for the High Temperature Diffusion-Bonded Compact Heat Exchangers," Proceedings of ICAPP08, Anaheim, CA, Paper No. 8008.

[11] Manglik, R. M., and Bergles, A. E., 1995, "Heat Transfer and Pressure Drop Correlations for the Rectangular Offset Strip Fin Compact Heat Exchanger," Exp. Therm. Fluid Sci., **10**, pp. 171–180.

[12] Patankar, S. V., 1980, *Numerical Heat Transfer and Fluid Flow*, McGraw-Hill, New York.

[13] Kays, W. M., and London, A. L., 1984, *Compact Heat Exchangers*, McGraw-Hill, New York.

[14] Subramanian, S., 2005, "CFD Modeling of Compact Offset Strip-Fin High Temperature Heat Exchanger" M.S. thesis, UNLV, Las Vegas, NV.

[15] Hu, S., and Herold, K. E., 1995, "Prandtl Number Effect on Offset Fin Heat Exchanger Performance: Predictive Model for Heat Transfer and Pressure Drop," Int. J. Heat Mass Transfer, **38**(6), pp. 1043–1051.

[16] Haynes International, Inc., "Heat-Resistant Alloy-at-a-Glance: Haynes 617 Alloy," http://www.haynesintl.com

[17] Yin, J., and Jensen, M. K., 2003, "Analytic Model for Transient Heat Exchanger Response," Int. J. Heat Mass Transfer, **46**, pp. 3255–3264.

[18] Romie, F. E., 1984, "Transient Response of the Counterflow Heat Exchanger," ASME J. Heat Transfer, **106**(3), pp. 620–626.

[19] Roetzel, W., and Xuan, Y., 1992, "Transient Response of Parallel and Counterflow Heat Exchangers," ASME J. Heat Transfer, **114**(2), pp. 510–512.

[20] Boresi, A. P., and Schmidt R. J., 2003, *Advanced Mechanics of Materials*, 6th ed., Wiley & Sons, New York.

[21] Huang, W., Zhao, H., and Peterson, P. F., 2006, "Multi-Scale Stress Analysis for Compact Plate Heat Exchangers," 2006 International Congress on Advances in Nuclear Power Plants (ICAPP), Reno, NV.